Ecological Modelling 365 (2017) 80–92

Contents lists available at ScienceDirect

Ecological Modelling

journal homepage: www.elsevier.com/locate/ecolmodel

A dynamical systems framework for crop models: Toward optimal fertilization and irrigation strategies under climatic variability

Norman Pelak[a,b,*], Roberto Revelli[a,d], Amilcare Porporato[b,c]

[a] Department of Civil and Environmental Engineering, Duke University, 121 Hudson Hall, Box 90287, Durham, NC 27708, United States
[b] Department of Civil and Environmental Engineering, Princeton University, E-208 E-Quad, Princeton, NJ 08544, United States
[c] Princeton Environmental Institute, Princeton University, Princeton, NJ 08544, United States
[d] Department of Hydraulics, Transport, and Civil Infrastructures, Politecnico di Torino, Turin, Italy

ARTICLE INFO

Article history:
Received 29 August 2017
Received in revised form 5 October 2017
Accepted 6 October 2017
Available online 16 October 2017

Keywords:
Crop model
Agroecosystems
Nitrogen
Fertilization
Dynamical systems

ABSTRACT

Crop models are widely used for the modeling and prediction of crop yields, as decision support tools, and to develop research questions. Though typically constructed as a set of dynamical equations, crop models are not often analyzed from a specifically dynamical systems point of view, despite its potential to elucidate the roles of feedbacks and internal and external forcings on system stability and the optimization of control protocols (e.g., irrigation and fertilization). Here we develop a minimal dynamical system, based in part on the widely known AquaCrop model, consisting of a set of ordinary differential equations (ODE's) describing the evolution of canopy cover, soil moisture, and soil nitrogen. These state variables are coupled through canopy growth and senescence, the evapotranspiration and percolation of soil moisture, and the uptake and leaching of soil nitrogen. The system is driven by random hydroclimatic forcing. Important crop model responses, such as biomass and yield, are calculated, and optimal yield and profitability under differing climate scenarios, irrigation strategies, and fertilization strategies are examined within the developed framework. The results highlight the need to maintain the system at or above resource limitation thresholds to achieve optimality and the role of system variability in determining management strategies.

1. Introduction

As tools to forecast or backcast crop yields, improve management strategies, and better understand the physical processes underlying crop production, crop models are important tools from both a research and an engineering viewpoint (Wallach et al., 2006; Steduto et al., 2009). The model outputs, structure, parameterization, and data assimilation are all active areas of crop modeling research. Because different users have different goals, several types of crop models have been proposed, which can be categorized in a number of ways. One of the most basic distinctions is between dynamic crop models, which are comprised of a set of differential equations, which are then integrated in time to simulate the crop responses of interest at each time point (often daily), and crop response models, which, though they may be built on dynamic models, relate crop responses directly to inputs (Thornley and Johnson, 1990; Wallach et al., 2006). Most crop models have as their main state variables above-ground biomass, leaf area index (LAI), harvestable yield, and water and nitrogen balances, though the choice and precise number of state variables varies (Wallach et al., 2006). Virtually all crop models are process-based, but necessarily involve empirical components, and are of varying levels of complexity, depending on the particular goals of the model and on the availability of input data. Some are specific to certain crops or groups of crops, such as CERES (Ritchie et al., 1998) and AZODYN (Jeuffroy and Recous, 1999), while others are more generic, such as CROPGRO (Boote et al., 1998), CROPSYST (Stöckle et al., 2003), STICS (Brisson et al., 2003), and some focus on particular regions (e.g., INFOCROP (Aggarwal et al., 2006) for tropical regions). Also in the category of generic models, but with a more parsimonious framework, is AquaCrop (Steduto et al., 2009). Despite the abundance of crop models which have dynamical systems at their core, they are not often analyzed as dynamical systems *per se* – that is, using the wide array of tools and methods provided by dynamical systems theory to understand the mathematical behavior and properties of the models (Strogatz, 2014). There are a number of potential reasons for this, such as the difficulty of applying these

* Corresponding author.
E-mail addresses: norman.pelak@duke.edu (N. Pelak), roberto.revelli@polito.it (R. Revelli), aporpora@princeton.edu (A. Porporato).

https://doi.org/10.1016/j.ecolmodel.2017.10.003
0304-3800/

methods to complex models and the aims of modelers, which may be focused toward other goals.

Although they tend to be considerably more complex and serve different purposes, crop models share many features and describe many of the same processes as do minimal ecohydrological models. The use of such models, which are typically formulated as dynamical systems, has provided many insights into soil moisture dynamics, plant–water interactions, and nutrient cycling (Rodríguez-Iturbe et al., 1999; Porporato et al., 2002, 2003; Rodríguez-Iturbe and Porporato, 2004). Some features of this type of ecohydrological model, such as the parsimonious representation of processes and stochastic and dynamic coupling between state variables, are well-suited to study the feedbacks, nonlinearities, and effect of random hydroclimatic forcing on agroecosystems (Porporato et al., 2015). Indeed, the underlying assumptions of many dynamic ecohydrological models are better met in agroecosystems than in the natural ecosystems where they are normally applied. Such assumptions include homogenous soil depth and plant spacing, as well as good drainage, which describe well an agricultural field with tillage, uniform crop spacing, and tile drains.

Various studies have used a dynamical systems framework to examine grass ecosystems (Thornley and Verberne, 1989; Tilman and Wedin, 1991), grass growth modulated by competition with legumes (Thornley et al., 1995) and grazing (Johnson and Parsons, 1985), forest ecosystems (Thornley and Cannell, 1992), forest ecosystems under harvest (Parolari and Porporato, 2016), soil salinity and sodicity (Mau and Porporato, 2015), and the cycles themselves, including feedbacks and nonlinearities (Porporato et al., 2003; Manzoni et al., 2004; Manzoni and Porporato, 2007). Studying crop models with dynamical systems theory allows for the more ready exploration of many interesting aspects of crop systems, including their stability with respect to parameter change, the feedbacks between water, carbon, and nutrient cycling, the optimal conditions for growth, and the impact of external inputs such as changes in climate patterns and management choices (i.e. fertilization and irrigation).

With the goal of taking advantage of the tools of dynamical systems theory, in this work we develop a dynamic crop model which captures the main crop fluxes and responses of interest without being overly complex. The model has three main variables which interact dynamically: the canopy cover, the relative soil moisture, and the soil nitrogen. The differential equations which account for these components are coupled via the crop growth, nitrogen uptake and leaching, and evapotranspiration terms. Biomass and yield, which are not considered to interact dynamically with the other state variables but rather are determined by them, are also included as derived variables of agroecologic interest. The model is used to examine the crop response to water and nutrient availability and varying climatic conditions in order to examine questions of optimal fertilization and irrigation and reduction of nutrient leaching.

Several aspects of the model are derived from AquaCrop (Steduto et al., 2009; Raes et al., 2009; Hsiao et al., 2009), which is the existing generic crop model that, in addition to its parsimony, can perhaps most easily be viewed as a dynamical system. It is also physically based, validated for a variety of crops, and widely known. AquaCrop itself is largely based on earlier FAO publications, in particular through its use of crop coefficients (Allen et al., 1998) and in the relation between crop water uptake and yield (Doorenbos and Kassam, 1998). The most notable similarities between the model developed here and AquaCrop are that canopy cover is used rather than the more typical LAI, that evapotranspiration is represented by crop coefficients, and in the dependence of the partitioning of transpiration and evaporation on the canopy cover. Some key differences involve the soil moisture balance (the model developed here makes use of a single vertically averaged soil moisture value rather than a soil column consisting of multiple layers, and it uses the same soil moisture stress thresholds throughout) and the nitrogen balance (a balance of total mineral nitrogen in the soil is used here rather than the empirical fertility coefficient employed in AquaCrop).

Here a different viewpoint and set of tools is emphasized for studying dynamic crop models, and we also aim to place crop models in a dynamical systems context and to discuss the application of the associated methods to crop models. We hope that this contribution will be of interest to both the crop modeling community and to researchers in the area of theoretical ecohydrology as a means to explore the response of agroecosystems to uncertain climatic conditions and optimal management strategies.

2. Model components

In this section a dynamical system is constructed which describes the interaction of three main components: canopy cover $C(t)$, relative soil moisture $S(t)$, and total nitrogen content in the soil $N(t)$. We also consider two related variables, namely the crop biomass $B(t)$ and the crop yield $Y(t)$ (hereafter we drop the t-dependence of the state variables). The model is interpreted at the daily timescale (no diurnal dynamics are considered) and applied over the course of a single growing season. It can be forced by random rainfall inputs (Rodríguez-Iturbe and Porporato, 2004), and is assumed to apply to an agricultural field which is homogenous in terms of soil composition, climatic forcing, and management.

2.1. Canopy cover dynamics

We define the canopy cover to be the fraction of ground covered by a crop. The benefit of using this alternative to the LAI, which was also employed by AquaCrop (Steduto et al., 2009), is that it combines multiple attributes of the crop canopy into a single, easily measured or estimated variable. The rate of change in canopy cover is modeled as a balance between the increase due to canopy growth and the decrease due to metabolic limitations and senescence, so that

$$\frac{dC}{dt} = G(C, S, N, t) - M(C, t), \tag{1}$$

where G is the canopy growth rate, and M is a term which combines the effects of metabolic limitation and senescence. The growth rate is assumed to be proportional to the rate of nitrogen uptake, U (discussed further in Section 2.3), giving

$$G(C, S, N, t) = r_G \cdot U(C, S, N, t), \tag{2}$$

where r_G is the canopy cover increase per amount of nitrogen taken up (the value for this and other crop growth parameters can be found in Table 1). The combined metabolic limitation and mortality/senescence term is

$$M(C, t) = (r_M + \gamma(t - t_{sen}) \cdot \Theta(t - t_{sen})) \cdot C^2, \tag{3}$$

where the first term, r_M, is a constant metabolic limitation term, and the next term is a time-dependent mortality and senescence term. For the latter, a linear function is used which increases with a slope of γ after the senescence onset time, t_{sen}, at which point the Heaviside step function, Θ, causes the senescence term to begin to affect the equation. This form recalls somewhat the Gompertz–Makeham law (Makeham, 1860), which includes an age-independent mortality term and an age-dependent mortality term, although here the constant term is conceptualized as a metabolic limitation term and the time-dependent term as a senescence term. For unstressed conditions (sufficiently high S and N) prior to t_{sen}, Eq. (1) is the logistic growth equation (Murray, 2002), and it includes the approximately exponential growth of C in the initial growth stage, the slowing of

Table 1
Model parameters.

Parameter	Value	Units	Name/description	Source
r_G	560	m^2/kg N	Canopy growth per unit N uptake	Calculated using data from Hsiao et al. (2009)
r_M	0.2	1/d	Canopy decline due to metabolic limitation	Calculated using data from Hsiao et al. (2009)
γ	0.005	$1/d^2$	Slope of increase of senescence after t_{sen}	Calculated using data from Hsiao et al. (2009)
K_{cb}	1.03	–	Max. T/ET_0	
K_{ce}	1.1	–	Max. E/ET_0	Hsiao et al. (2009)
t_{sen}	110	d	Days until onset of senescence	Mean of values in Table 2 of Hsiao et al. (2009)
t_{GS}	140	d	Length of growing season	Mean of values in Table 2 of Hsiao et al. (2009)
W^*	3.37×10^{-2}	kg B/m^2/d	Normalized daily water productivity	Hsiao et al. (2009)
h	0.5	kg Y/kg B	Maximum harvest index	Hsiao et al. (2009)
η_c	0.054	kg N/m^3 water	Maximum N concentration taken up	Derived from model parameters
D	5.5×110^{-6}	kg/m^2/d	N deposition rate	National Atmospheric Deposition Program (NRSP-3) (2017)
F_t	0.0286	kg N/m^2	Maximum N uptake	Bender et al. (2013)
p_Y	0.12	$/kg	Corn price per kg of yield	Lamm et al. (2007)
p_F	0.639	$/kg	Fertilizer unit price N	Lamm et al. (2007)
p_I	0.0148	$/$m^3$	Irrigation water unit price	Vico and Porporato (2011b)
p_L	0	$/kg	Cost of leached N	Set to 0 in current simulations
p_{fix}	0.109	$/$m^2$	Fixed costs	

growth as a limit is reached, and the negligible growth rate near the carrying capacity. This compares well with the data for canopy cover presented by Hsiao et al. (2009) (see Section 3.1).

2.2. Soil moisture balance equation

Soil moisture is modeled as a balance between gains from rainfall and irrigation and losses to evapotranspiration and leakage (Rodríguez-Iturbe and Porporato, 2004; Vico and Porporato, 2010)

$$\phi Z \frac{dS}{dt} = R(t) + I(S,t) - T(S,C,t) - E(S,C,t) - L(S), \tag{4}$$

where S is the vertically averaged relative soil moisture, ϕ is porosity, and Z is a soil depth with homogenous characteristics (Table 2 contains values for the soil parameters). ϕZ is defined as the active soil depth (Laio et al., 2001b), the volume per surface area available for water storage. In agricultural soils, tilling tends to rearrange soil profiles so that the top layer of soil is relatively uniform in composition and depth. We assume that the root growth (which we do not explicitly model) is constricted to Z, and that hydraulic redistribution over this depth allows water to easily move to areas of lower soil moisture, making the vertically-averaged soil moisture a good description of the amount of water available for evapotranspiration (Guswa et al., 2002).

R is the rainfall rate. For the purposes of a probabilistic analysis, here it is modeled as a marked Poisson process with mean event frequency λ and exponentially distributed rainfall events depths α (Rodríguez-Iturbe and Porporato, 2004). This stochastic component allows for the model to include the effect of unpredictable external forcing via rainfall, which is especially important in arid and semi-arid ecosystems, and for rain-fed agriculture.

In the case of irrigated agriculture, a term I gives the irrigation rate, which may be a function of S and/or t depending on the irrigation strategy employed (e.g., stress avoidance or microirrigation) (Vico and Porporato, 2010, 2011a,b).

The transpiration rate T is assumed to be proportional to C and is given by

$$T(S,C,t) = K_s(S) \cdot C \cdot K_{cb} \cdot ET_0(t), \tag{5}$$

where $K_s(S)$ is a water stress coefficient, K_{cb} is a basal crop coefficient (essentially the midseason basal crop coefficient of Allen et al. (1998)), and ET_0 is the reference evapotranspiration, which is calculated using the Penman–Monteith equation for a reference crop (normally grass, but occasionally alfalfa) (Allen et al., 1998). As no diurnal variation is considered, ET_0 is a mean daily rate and thus the model should be interpreted at the daily timescale. The water stress coefficient is given by

$$K_s(S) = \begin{cases} 0 & S \le S_w, \\ \dfrac{S - S_w}{S* - S_w} & S_w < S \le S*, \\ 1 & > S* < S, \end{cases} \tag{6}$$

where S_w is the wilting point and S^* is the point of incipient stomatal closure. $K_s(S)$ therefore captures the plant stomatal response to soil moisture conditions. As mentioned previously, the plant is assumed to be able to easily compensate for areas of low soil moisture in the soil column by drawing more water from areas of high soil moisture, making S a good indicator of the amount of water available to the plant. However, this assumption is weakened if the plant cannot do so because of high root resistance or spatial heterogeneities in the soil properties (Guswa et al., 2002).

The evaporation rate E is assumed to be proportional to $(1 - C)$ and is given by

$$E(S,C,t) = K_r(S) \cdot (1 - C) \cdot K_{ec} \cdot ET_0(t), \tag{7}$$

where $K_r(S)$ reduces evaporation according to soil moisture and K_{ec} is a baseline evaporation coefficient. A similar dependence of evaporation on $1 - C$ was used by Steduto et al. (2009). The evaporation reduction coefficient is given by

$$K_r(S) = \begin{cases} 0 & S \le S_h, \\ \dfrac{S - S_h}{1 - S_h} & S \ge S_h, \end{cases} \tag{8}$$

where S_h is the hygroscopic point, below which no soil moisture losses occur. A diagram of K_s and K_r as a function of S is shown in the upper panel of Fig. 1, and the increase of evapotranspiration as a whole with increasing S can be seen from top to bottom in the lower panel of Fig. 1. Evaporation draws primarily from a thin top layer of soil, drawing from lower soil layers only when potential gradients drive water from lower soil depths upward. This is often modeled using the two stage method for soil evaporation (Ritchie, 1972; Brutsaert and Chen, 1995). The dependence of E on the average soil moisture value over a depth Z simplifies the actual relationship, but it does capture the high rates of evaporation at saturation ($S = 1$) and the trend toward a rate of zero evaporation as S approaches S_h. The form that is used for K_s is essentially equivalent to the expression for transpiration used in Laio et al. (2001b), while the form for K_r is quite different from that used for evaporation in the same paper. Laio et al. (2001b) considered evaporation and transpiration separately, with the former being very small due to the presence of

Table 2
Climate and soil parameters.

Parameter	Value	Units	Name/description	Source
α	1.5	cm	Mean rainfall depth	Sample values
λ	0.3	1/d	Mean rainfall frequency	Sample values
ET_0	5×10^{-3}	m/d	Reference evapotranspiration	Approximated from Hsiao et al. (2009)
S_h	0.14	–	Hygroscopic point	Rodríguez-Iturbe and Porporato (2004)
S_w	0.17	–	Wilting point	Rodríguez-Iturbe and Porporato (2004)
S^*	0.35	–	Point of incipient stomatal closure	Rodríguez-Iturbe and Porporato (2004)
S_{fc}	0.59	–	Field capacity	Rodríguez-Iturbe and Porporato (2004)
k_{sat}	0.33	m/d	Saturated hydraulic conductivity	Rodríguez-Iturbe and Porporato (2004)
d	13	–	Leakage parameter	Rodríguez-Iturbe and Porporato (2004)
a	~1	–	Fraction of N dissolved	Porporato et al. (2003)
ϕ	0.43	–	Soil porosity	Rodríguez-Iturbe and Porporato (2004)
Z	1.0 m	d	Soil depth	Irmak and Rudnick (2014)

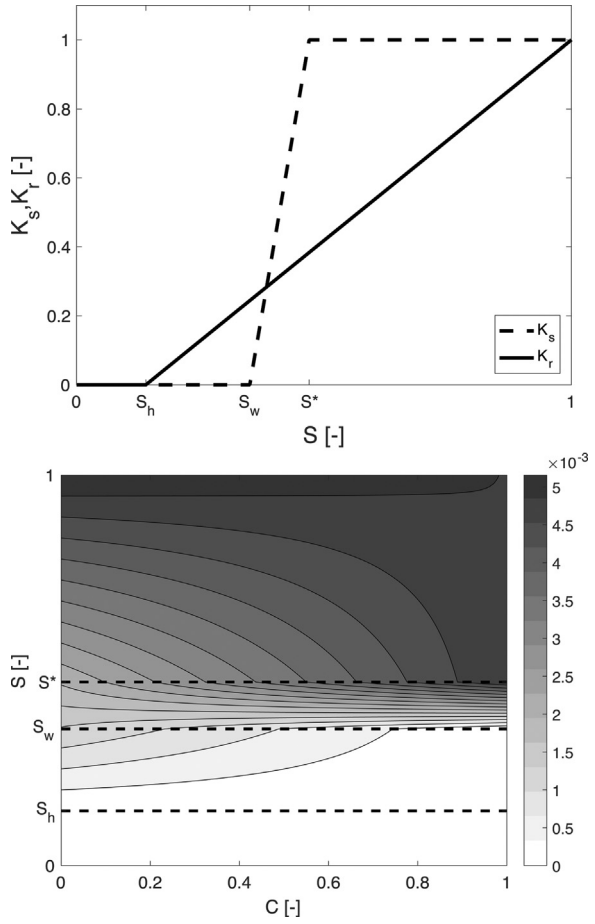

Fig. 1. Top: the water stress coefficient (dashed line) and the evaporation reduction coefficient (solid line) as a function of soil moisture S. Bottom: evapotranspiration [m/d] as a function of S and C, with values of ET_0 and the soil moisture thresholds as in Table 1.

the plant canopy. However, as we are interested in the crop canopy as it develops throughout the growing season (from left to right in the lower panel of Fig. 1), the maximum values for T and E must be of somewhat similar magnitude to capture the dominance of E shortly after planting and that of T later in the growing season (this is reflected in the fact that K_{cb} and K_{ce} are indeed nearly the same) (Kelliher et al., 1995).

The combined percolation and runoff rate is denoted as Q, and as we are considering well-drained agricultural fields, subsurface percolation is assumed to dominate compared to overland runoff and to be equal to the hydraulic conductivity, i.e.,

$$Q(S) = k(S) = k_{sat} \cdot S^d, \tag{9}$$

where k is the hydraulic conductivity, k_{sat} is the saturated hydraulic conductivity, and d is an empirically based parameter (Brooks and Corey, 1964; Rodríguez-Iturbe and Porporato, 2004).

2.2.1. Calculation of S_w and S^*

Using data for silty loam (a common agricultural soil) and methods from Clapp and Hornberger (1978) and Laio et al. (2001a), the wilting point S_w of was calculated as the soil moisture level corresponding to a matric potential of −1.5 MPa. Corn begins to suffer water stress when approximately 50% of the total available water (which is the water content at field capacity minus that at the wilting point) is depleted (Rhoads and Yonts, 2000). Therefore, we calculate the point of incipient stomatal closure S^* as $S* = (S_w + S_{fc})/2$. For silty loam, $S_w = 0.35$, S^* =0.47, and S_{fc} = 0.59.

2.3. Soil nitrogen content

While AquaCrop (Steduto et al., 2009) makes use of an empirical measure of soil fertility that allows the model to be used even if detailed soil nitrogen data are not available, most crop models consider a nitrogen balance (Ritchie et al., 1998; Jeuffroy and Recous, 1999; Boote et al., 1998; Stöckle et al., 2003; Brisson et al., 2003; Aggarwal et al., 2006) due to its key role in the growth and development of crops. In order to better examine crop growth and yield under optimal fertilization and irrigation strategies, a soil nitrogen balance is also included here. The evolution of total mineral nitrogen in the soil is given by the balance between deposition and fertilization as inputs and leaching and plant uptake as outputs (Porporato et al., 2003)

$$\frac{dN}{dt} = D(t) + F(N,t) - L(S,N) - U(S,N,C,t), \tag{10}$$

where N is nitrogen content per unit area of soil, D is the rate of natural nitrogen addition to the soil, and F is the fertilization rate. For all figures in this paper, the average annual rate of nitrogen deposition for a heavily agricultural region has been used as a constant deposition rate D (National Atmospheric Deposition Program (NRSP-3), 2017). Unless otherwise noted, the fertilization rate F is considered to be the maximum potential uptake of nitrogen F_t divided by the length of the growing season, t_{GS}. The total mineral nitrogen content in the soil, rather than the individual nitrate and ammonium components, is used because plants are able to take up both forms, making the separation of the two unnecessary in the case of this model, which aims for a general picture of nitrogen fluxes.

The leaching term L is proportional to the percolation from the hydrologic balance, Q, and the nitrogen concentration as

$$L(S,N) = \frac{aN}{S\phi Z} Q(S), \tag{11}$$

where a is the fraction of N which is dissolved in the soil moisture ($a \approx 1$ for nitrate, while $a \leq 1$ for ammonium). The nitrogen concen-

tration in the soil moisture is given by the quantity $\frac{aN}{S\phi Z}$, which is denoted by η.

Plant uptake of nitrogen, U, is given by

$$U(S, N, C, t) = f(\eta) \cdot T(S, C, t), \tag{12}$$

in which $f(\eta)$ is a function which limits the nitrogen uptake above a certain critical concentration η_c, with the form

$$f(\eta) = \begin{cases} \frac{aN}{S\phi Z} & \frac{aN}{S\phi Z} < \eta_c, \\ \eta_c & \frac{aN}{S\phi Z} \geq \eta_c. \end{cases} \tag{13}$$

The physical reasoning for this limitation is that beyond a certain point, taking up more nitrogen is not useful for the plant to increase its growth rate, and extremely high nitrogen concentrations in plant tissue are toxic to the plant. The above limitation is meant to account in a parsimonious way for the plant's ability to exclude nitrogen from transpired water (i.e. active uptake (Porporato et al., 2003)). It is worth noting that a reduction in S can either increase or decrease the N uptake. As long as $S > S^*$, a reduction in S increases the concentration η, thereby increasing N uptake if initially $\eta < \eta_c$. However, if S drops below S^*, transpiration decreases and therefore so does N uptake.

2.4. Crop biomass and yield

While the dynamics of the model are contained in the equations for C, S, and N, other variables which depend on one of the three main variables are also of interest. Specifically, we consider the crop biomass B and crop yield Y.

The accumulation of plant biomass is modeled using the normalized daily water productivity W^* (e.g., Steduto et al. (2009)), which is typically multiplied by the ratio of transpiration to reference evaporation to model biomass accumulation. However, in place of transpiration we us the nitrogen uptake divided by the nitrogen uptake threshold η_c, giving

$$\frac{dB}{dt} = W* \frac{U(S, N, C, t)}{\eta_c ET_0(t)} = \frac{W*}{\eta_c} K_s(S) K_{cb} f(\eta) C. \tag{14}$$

The use of $\frac{U}{\eta_c}$ rather than T allows us to extend the concept of water productivity to also consider the effects of nitrogen limitation. When $\eta \geq \eta_c$, one recovers the biomass growth equation used by Steduto et al. (2009) and others, which considered transpiration rather than nitrogen uptake for biomass accumulation.

The biomass and yield are related through a harvest index, h, which is the fraction of the biomass which makes up the yield. The harvest index is often modeled as an increasing function in time which is modulated by various stresses (Steduto et al., 2009; Raes et al., 2009). Here we instead utilize a reference value for h and assume that stress limitations are sufficiently accounted for elsewhere in the crop growth equations, recognizing that this limits the validity of the crop yield calculations to the end of the growing season. The yield is then

$$Y = h \cdot B. \tag{15}$$

3. Reduced versions of the model

The complete model is defined by the balance equations for C, S, and N (Eqs. (1), (4), and (10)) and their component fluxes, with Eqs. (14) and (15) defining additional variables. Two reduced versions of the model will now be examined. The first, in which S and N are held constant, is compared to canopy cover data to estimate parameters for Eq. (1). The second, in which only S is held constant (and there is therefore no stochastic forcing), is analyzed as a typical deterministic dynamical system in order to demonstrate some of the insights which can be gained from this approach.

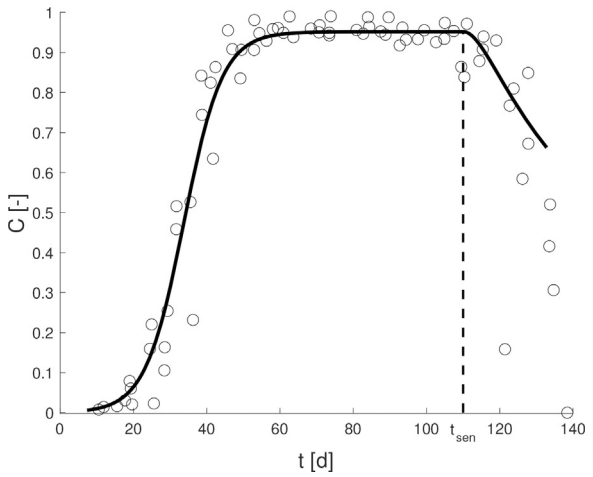

Fig. 2. Growth of canopy cover in the C-only model, using the parameterization as described in the text (black line). Data are from 6 years of maize experiments in Davis, CA (Hsiao et al., 2009) (open circles).

3.1. Canopy growth equation and its parameterization

We begin by examining the simplest version of the model, in which S and N are fixed (at $S \geq S^*$ and with N such that $\eta \geq \eta_c$) but C is allowed to vary. In these conditions (and also with ET_0 constant, to maintain analytical tractability), Eq. (1) reduces to

$$\frac{dC}{dt} = r_G K_{cb} ET_0 \eta_c \cdot C - (r_M + \gamma(t - t_{sen}) \cdot \Theta(t - t_{sen})) \cdot C^2, \tag{16}$$

which is simply the logistic model if $t < t_{sen}$, in which case this equation can be solved analytically as

$$C(t) = \frac{r_G K_{cb} ET_0 \eta_c C_0 e^{r_G K_{cb} ET_0 \eta_c t}}{r_G K_{cb} ET_0 \eta_c + C_0 r_M \left(e^{r_G K_{cb} ET_0 \eta_c t} - 1\right)}, \tag{17}$$

which is the logistic equation (Murray, 2002).

In order to parameterize Eq. (16), it was necessary to use data from a growing season in which the crop did not experience water or nitrogen stress. Values for r_G, r_M, and γ have therefore been obtained by minimizing the RMSE of the model compared to the data from Hsiao et al. (2009) for fully irrigated and fertilized conditions. The data come from 6 seasons of experiments spread over 22 years in Davis, CA. The first three years used slightly different maize cultivars, while the last three used the same cultivars, but in order to include more data they have been assumed to be similar enough to consider together. An approximate mean reference evapotranspiration rate ET_0 and the value for K_{cb} were also taken from Hsiao et al. (2009). These experiments did not report soil N or uptake rates, and so η_c has been estimated by averaging the cumulative N uptake for maize found in Bender et al. (2013) across the growing season. While it would be preferable to use a more complete single dataset for the model parameterization, the emphasis here is not on predicting crop growth but on reproducing the general crop behavior. Fig. 2 shows the model vs. the data against which it was parameterized, demonstrating a good fit particularly prior to the time of senescence, t_{sen}. The value for t_{sen} is cultivar-specific and for this figure was taken as the average t_{sen} over the 6 years of experiments. The value of this parameter and all others discussed in this section can be found in Table 1.

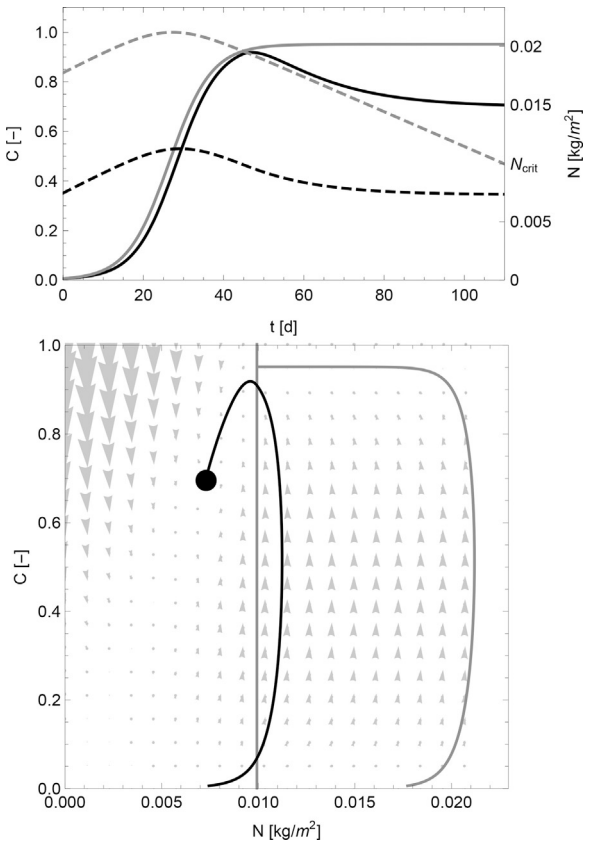

Fig. 3. Top: timeseries of canopy cover and soil nitrogen for the *C*–*N* model, for two differing initial conditions of *N* (solid lines represent *C*; dashed lines represent *N*). Bottom: *C*–*N* vector plot and phase portrait, for two initial conditions. The black dot represents the stable fixed point (N_2, C_2), and the solid gray line is the η_c threshold. Note that in this figure, the combined fertilization and deposition rate has been reduced slightly in order to better show the impact of varying the initial conditions, and the simulation has only been performed until t_{sen} because after this point in time the trajectories no longer converge towards the same fixed point.

3.2. N *and* C *system*

An interesting 2-D dynamical system is obtained when *C* and *N* are free to vary in time, but *S* is kept constant, which approximates the conditions in an agricultural field with a microirrigation system and constant fertilization and deposition rate, $F + D = F_0$. The top panel of Fig. 3 shows the evolution of the two state variables *N* and *C* in time, while the bottom panel is a phase space diagram which shows sample trajectories in the *C*–*N* phase space. It is easy to see the development of the state variables for different initial conditions, and the effects of parameter changes on the vector field, which determines the direction the system moves for a given condition, can also be examined using this type of diagram. In the bottom of Fig. 3, the η_c threshold of Eq. (13) can be seen as the solid gray line which separates the two parts of the solution – on the left side, $\eta < \eta_c$, and on the right, $\eta > \eta_c$. Optimization will be further discussed in a later section, but for now we point out that in order to maximize crop growth, the system should be kept on the right side of this threshold, as the trajectories of the vector field here point to higher values of *C* and thereby greater rates of crop growth.

Different solutions exist above and below η_c because when $\eta \geq \eta_c$, sufficient nitrogen is available for crop growth, and Eq. (1) is decoupled from *N*. An analytic expression for $C(t)$ can be obtained (when $t < t_{sen}$) due to this decoupling, which is shown in Eq. (17). An exact expression can also be found for $N(t)$, but as it is rather involved it is not included here. When $\eta < \eta_c$, the crop experiences nitrogen stress and Eq. (1) is again coupled to *N*. Analytical expressions for $C(t)$ and $N(t)$ are unavailable in this case.

3.2.1. *Fixed points and stability,* $\eta \geq \eta_c$

For the simpler case of $\eta \geq \eta_c$ and $t < t_{sen}$, the first fixed point is given by

$$C*_1 = 0, \tag{18}$$

$$N*_1 = \frac{F_0 \cdot S\phi Z}{a \cdot k_{sat} S^d}, \tag{19}$$

while the expressions for the second are

$$C*_2 = \frac{r_G}{r_M} K_{cb} E T_0 \eta_c, \tag{20}$$

$$N*_2 = \frac{S\phi Z\left(F_0 - \frac{r_M}{r_G} C_2^{*2}\right)}{a \cdot k_{sat} S^d} = \frac{S\phi Z\left(F_0 - \frac{r_G}{r_M} K_{cb}^2 E T_0^2 \eta_c^2\right)}{a \cdot k_{sat} S^d}. \tag{21}$$

Recalling Eq. (1) with $\frac{dC}{dt} = 0$, we note that the steady-state uptake of nitrogen is given by $\frac{r_M}{r_G}(C_2^{*2}) = \frac{r_G}{r_M} K_{cb}^2 E T_0^2 \eta_c^2$, a quantity which can also been seen inside the parentheses in Eq. (20). The first fixed point is an unstable node and the second is a stable node (a third exists, but it is always negative and thus not physical). The eigenvalues of the first fixed point are

$$\lambda_{1a} = -\frac{a \cdot k_{sat} S^d}{S\phi Z}, \tag{22}$$

$$\lambda_{1b} = E T_0 \eta_c K_{cb} r_G, \tag{23}$$

while those of the second fixed point are

$$\lambda_{2a} = -\frac{a \cdot k_{sat} S^d}{S\phi Z}, \tag{24}$$

$$\lambda_{2b} = -E T_0 \eta_c K_{cb} r_G. \tag{25}$$

The first fixed point is always an unstable node, and in the second is always a stable node. This is unsurprising, as the standard logistic equation, which is contained within the system dynamics when $\eta \geq \eta_c$, likewise has one stable and one unstable node as its fixed points.

3.2.2. *Fixed points and stability,* $\eta < \eta_c$

If the system were allowed to develop to steady state ($t \to \infty$), the explicitly time-dependent part of the mortality $M(C, t)$ term would ultimately drive the canopy cover to a value of zero, and the soil nitrogen content would approach a value determined by the balance between the fertilization/deposition and leaching terms. The fixed points are obtained assuming no senescence term (e.g., if a perennial crop rather than an annual one were considered). In this condition, there are two fixed points. The first has the same expressions as Eqs. (18) and (19), while the second is

$$C*_2 = \frac{-k_{sat} S^d + \sqrt{(k_{sat} S^d)^2 + \frac{4F_0 \cdot E T_0^2 K_{cb}^2 r_G}{r_M}}}{2 E T_0 K_{cb}}, \tag{26}$$

$$N*_2 = \frac{-r_M Z \phi k_{sat} S^{d+1} + S\phi Z\sqrt{(r_M k_{sat} S^d)^2 + 4F_0 \cdot E T_0^2 K_{cb}^2 r_G}}{2 a E T_0^2 K_{cb}^2 r_G}. \tag{27}$$

The stability can more easily be seen when it is put in terms of the fertilization and deposition term, the critical value of which is derived from the expression for the eigenvalues and is given by

$$\begin{aligned} F_c = \; & 2aS^{2d} k_{sat}^2 r_M (aETK_{cb} - SZ\phi r_M) \\ & \cdot (a^2 E^2 T^2 K_{cb}^2 + 4aETSZ\phi K_{cb} r_M - S^2 Z^2 \phi^2 r_M^2) \\ & \div ETK_{cb} r_G (a^2 E^2 T^2 K_{cb}^2 - 6aETSZ\phi K_{cb} r_M + S^2 Z^2 \phi^2 r_M^2)^2, \end{aligned} \tag{28}$$

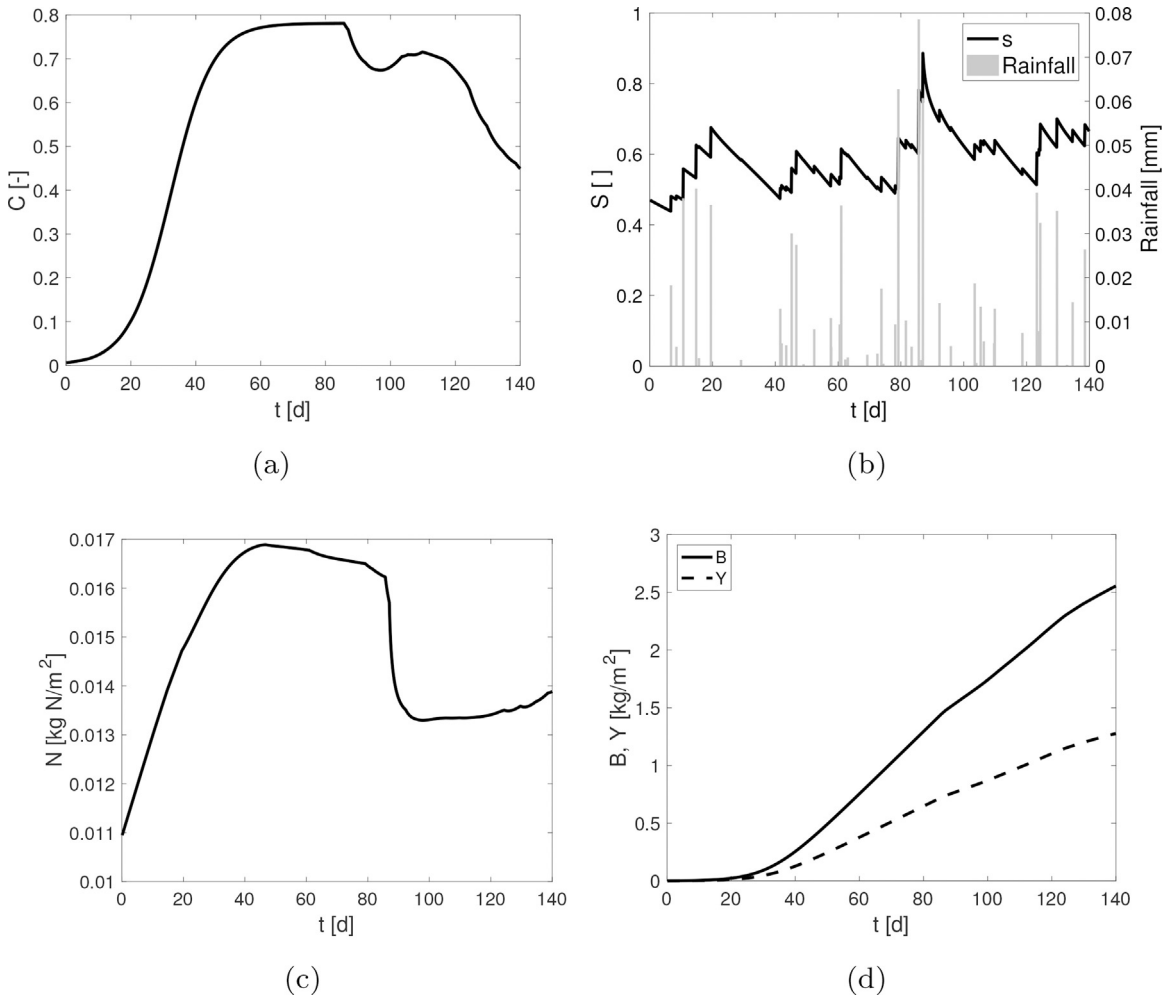

Fig. 4. Time series of (a) canopy cover C, (b) soil moisture S and rainfall R, (c) soil nitrogen N, (d) crop biomass and yield over a growing season.

so that the fixed point is a spiral when $F_0 < F_c$ and a node when $F_0 > F_c$, pointing to the possibility of damped oscillations. Oscillations related to nitrogen cycling were also observed by Thornley et al. (1995) (oscillations of LAI and soil nitrogen in a model of grass-legume dynamics), Tilman and Wedin (1991) (oscillations and possible chaos in interannual dynamics of a perennial grass), Manzoni and Porporato (2007) (shifts in stability in a model of substrate carbon and nitrogen dynamics), and Parolari and Porporato (2016) (stability shifts in a model of forest carbon and nitrogen cycles under harvesting). The interpretation of such oscillations is not entirely clear, as it is possible that they are merely artifacts of simplified models or the results of overfitting the available data, but their presence in such models is intriguing and deserves further attention.

4. Soil moisture dynamics and hydrologic forcing

The addition of the soil moisture dynamics greatly increases the model complexity, especially when the rainfall stochastic forcing is considered. This forcing adds considerable interest to the dynamics of the model, as it allows us to consider the effect of varying rainfall parameters as well as to examine the model in a probabilistic sense. While it is possible to obtain some analytic results regarding soil moisture probability distributions for statistically steady states under stochastic rainfall forcing (see for example Rodríguez-Iturbe and Porporato (2004)), the complexity of the crop growth function and nitrogen balance employed here make it necessary to proceed numerically (though see Schaffer et al. (2015) for a special case in which analytical results were obtained for stochastically driven soil moisture and plant biomass).

4.1. Soil moisture dry-down

Many important agroecosytems have some form of the Mediterranean climate, in which the rainfall occurs out of phase with the growing season. In this case, the soil moisture dynamics occur as a deterministic dry-down, with the exception of whatever small amounts of precipitation may occur during the growing season. Therefore, all other factors being equal, the crop yield of rainfed (i.e., non-irrigated) agriculture in this type of climate depends greatly on the initial condition of soil moisture that is available at the beginning of the growing season. Of course, this initial supply may also be supplemented by irrigation, which is similar to the case considered in Section 3.2.

4.2. Stochastic forcing

Figs. 4 and 5 show the development of the three main state variables and their associated fluxes over the course of a growing season, with $t = 0$ taken as the start of the growing season. Note that in these and the proceeding figures, a constant rate of nitrogen fertilization/deposition was imposed. As compared to the deterministic scenarios discussed in Section 3, the variables in the full model show much greater variability, due to the direct dependence

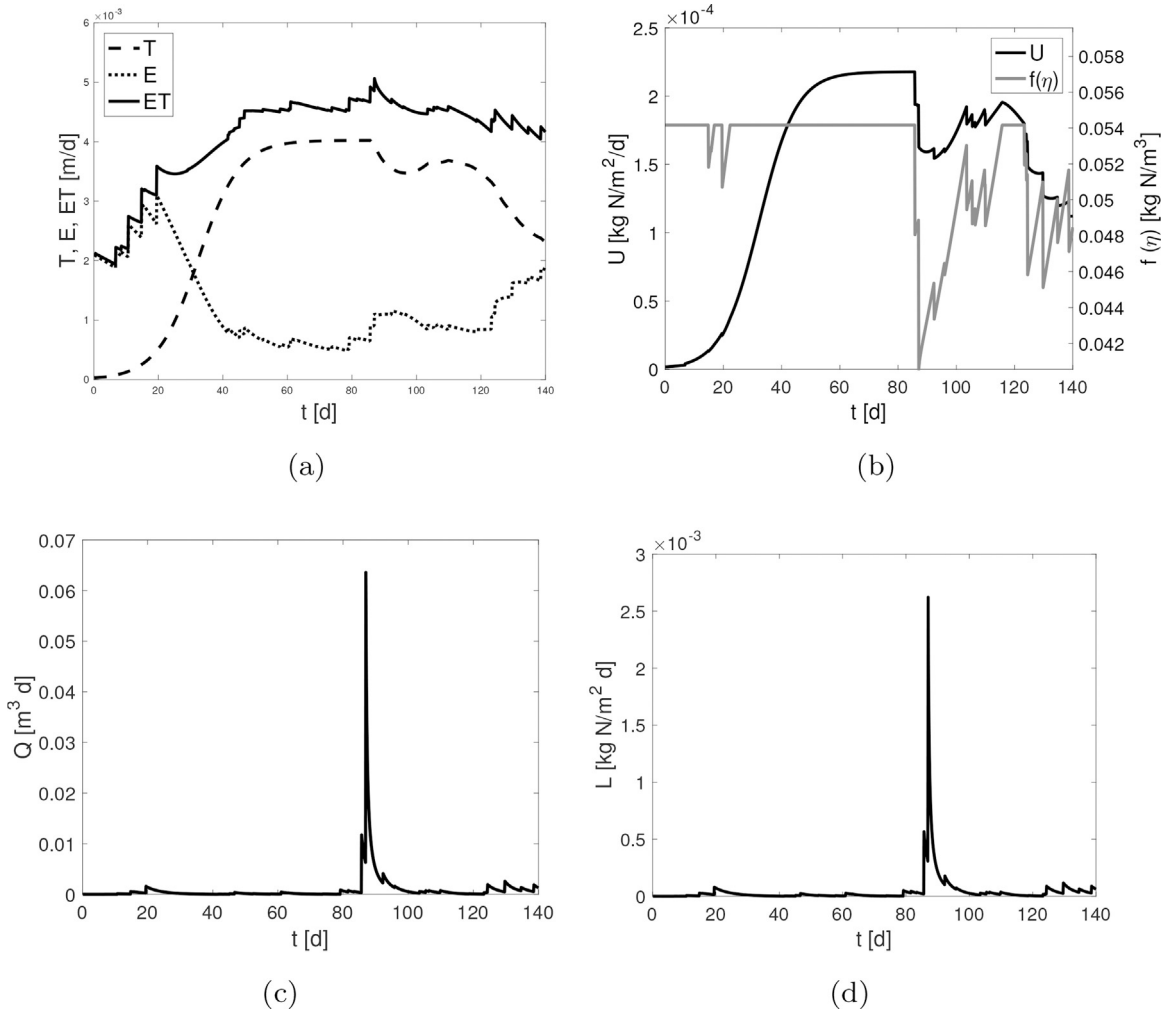

Fig. 5. Time series of (a) transpiration T, evaporation E, and evapotranspiration ET, (b) nitrogen uptake U and limitation function $f(\eta)$, (c) leakage Q, and (d) nitrogen leaching L.

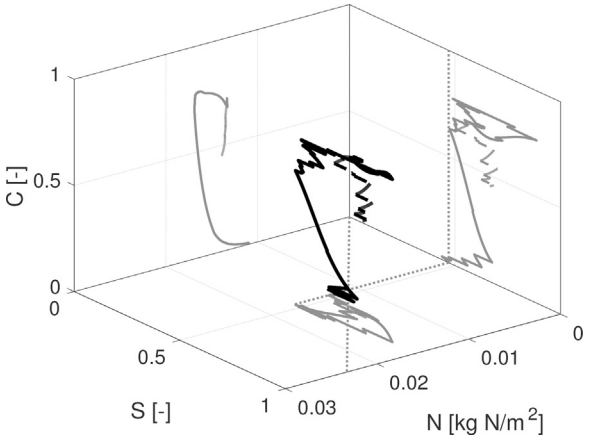

Fig. 6. A sample trajectory shown in the 3-dimensional phase space of C, S, and N (black line), and projections onto the three planes (gray lines). Dashed lines denote the dynamics which occur after t_{sen}, and the dotted lines the S^* threshold (S–C and S–N planes) and the η_c threshold (S–N plane).

of the fluxes on the stochastically driven soil moisture balance. Fig. 6 shows the main dynamic variables in the three-dimensional phase space. Observing this sample time series, excursions below the soil moisture threshold S^* (the dotted lines that are perpendicular to the S axis) and below the η_c threshold (the diagonal line on the S–N plane) can be seen to coincide with reductions in C. The case of water stress depends on S only, while the latter case of nitrogen stress involves the interaction of S and N because of their joint effect on the $f(\eta)$ limitation function.

4.3. Impact of rainfall regimes on rain-fed agriculture

The timing and amount of rainfall exerts a strong control on crop growth in rain-fed agriculture. We first examine the effect of different rainfall regimes when associated parameters (mean event depth α and mean frequency λ) are constant throughout a growing season, which is a reasonable approximation for growing season conditions in many regions of the world. Despite the fact that the parameters are constant in time, there remains a strong intra-seasonal time dependence, primarily due to the growth of canopy cover, C. This is due to both its growth in time and more explicitly through the time-dependence of the $M(C, t)$ term.

This pattern in time can be seen not only in Figs. 4 and 5 but also in Fig. 7, which shows the ensemble average over many simulations of canopy cover (top left), soil nitrogen (top right), soil moisture (bottom left), and nitrogen leaching (bottom right). In each simulation, the mean rainfall rate was kept constant but α and λ were changed, to demonstrate the interaction of rainfall event frequency and event size. Simulations with larger, less frequent events are characterized by reduced canopy cover, and higher rates of nitrogen leaching. However, there are also slightly higher levels of soil

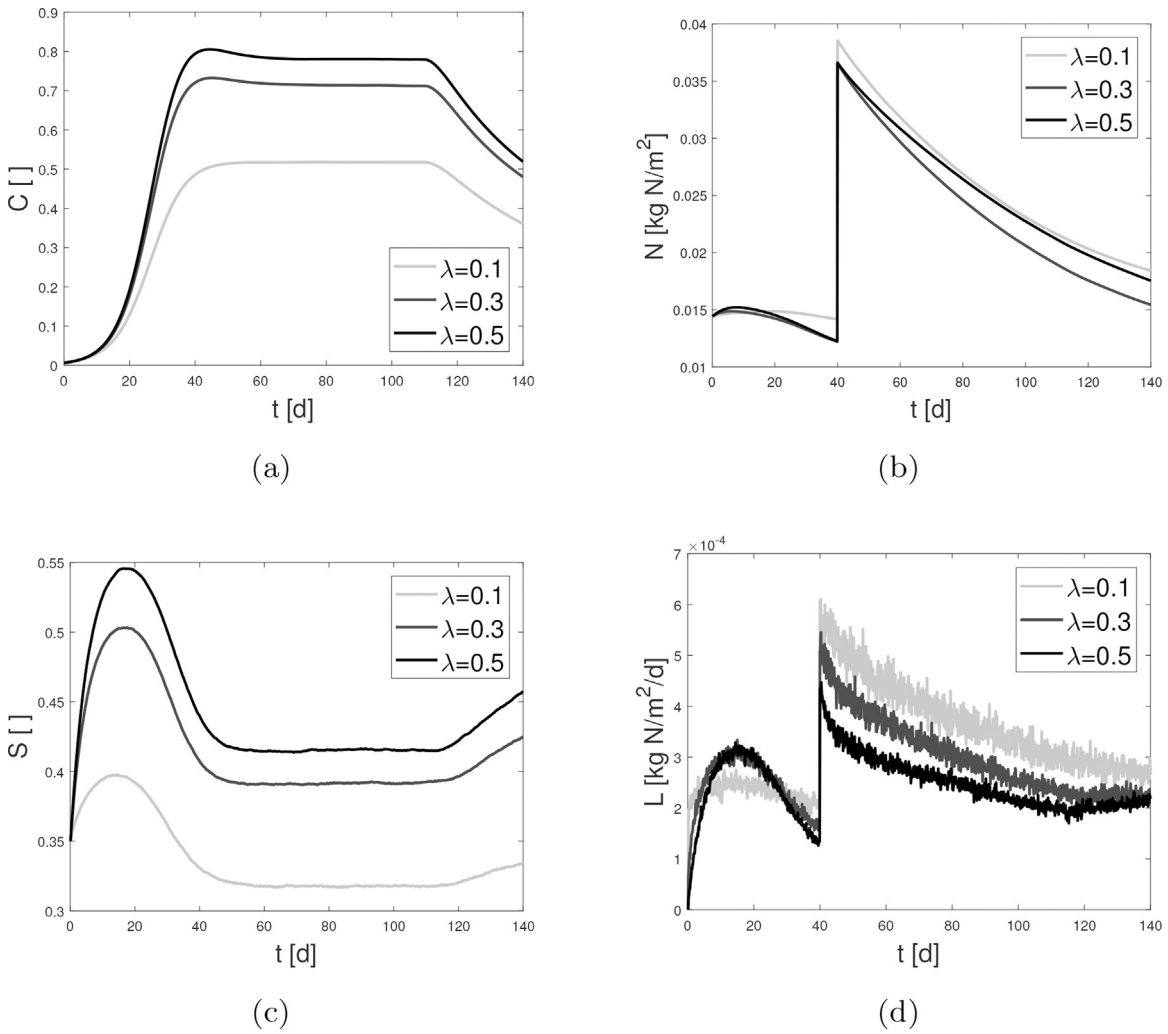

Fig. 7. A comparison of the mean (a) canopy cover, (b) soil nitrogen, (c), soil moisture, and (d) leaching across different precipitation regimes for $\lambda = 0.1\ d^{-1}$ (light gray), $\lambda = 0.3\ d^{-1}$ (gray), $\lambda = 0.5\ d^{-1}$ (black), with α altered to keep a constant mean rainfall rate of 4.5 mm/d for all figures. A typical fertilization treatment for corn has been applied, resulting in the observed jump in N.

nitrogen which remain, as the reduced soil moisture and canopy cover led to a low nitrogen uptake and thus higher soil moisture levels. The system shown in Fig. 7 undergoes a typical fertilization schedule for corn, in which some fraction ξ of the total fertilization F_t is applied at the beginning of the growing season, and the remainder is applied after a period τ, resulting in the jump which can be observed in N in Fig. 7b. Here, $\xi = 0.3$ and $\tau = 40$ d (see Section 5.1 and Fig. 10 for a discussion of the optimization of ξ and τ).

5. Optimal strategies

Crop models represent an important tool to study the impact of different management strategies aimed at maximizing yield, minimizing water and fertilizer use, reducing the leaching of fertilizers, and optimizing the timing of irrigation and fertilization treatments under hydroclimatic variability (Wallach et al., 2006). Toward this goal we develop a first-order objective function, which considers the profit from the sale of produce, costs of fertilizer and irrigation, 'environmental cost' of nitrogen leaching, and fixed costs,

$$P_{net} = p_Y \cdot Y(t_{GS}) - p_F \cdot F_{tot} - p_I \cdot I_{tot} - p_L \cdot L_{tot} - p_{fix}, \tag{29}$$

where p_Y [\$/kg Y] is the unit sale price of the crop yield at the end of the growing season, $Y(t_{GS})$. p_F [\$/kg N] and p_I [\$/m^3] are the unit prices of fertilizer and irrigation water, respectively, while the cumulative fertilization and irrigation are given by $F_{tot} = \int_0^{t_{GS}} F(N,t)dt$ and $I_{tot} = \int_0^{t_{GS}} I(S,t)dt$. The unit 'environmental cost' of leached nitrogen is given by p_L [\$/kg N], here conceptualized as the cost necessary to mitigate these losses or to pay associated fines, while the cumulative nitrogen leaching is given by $L_{tot} = \int_0^{t_{GS}} L(S,N)dt$. Finally, p_{fix} [\$/m^2] is a fixed cost representing distribution and energy costs, here estimated following Vico and Porporato (2011b). Estimated values for these parameters can be found in Table 1. This objective function should be thought of as a means to quantify the relative financial impact and importance of various components of the crop system, rather than as a way to obtain firm predictions about the profitability of various management strategies.

Fig. 8 shows several key crop responses under idealized, non-stochastic conditions. The responses of crop yield Y and the objective function P_{net} to different mean soil moisture and soil nitrogen conditions are illustrated in Fig. 8a and b. Fig. 8c and d shows the cumulative amounts of irrigation and fertilization, respectively, that would be needed to keep the S and N at the designated mean values. The horizontal lines mark the S^* threshold, below which point the transpiration begins to decrease, and the diagonal line marks the η_c concentration threshold.

Nitrogen use efficiency (NUE) is the ratio of the amount of nitrogen which is taken up by the crop to the amount which is applied,

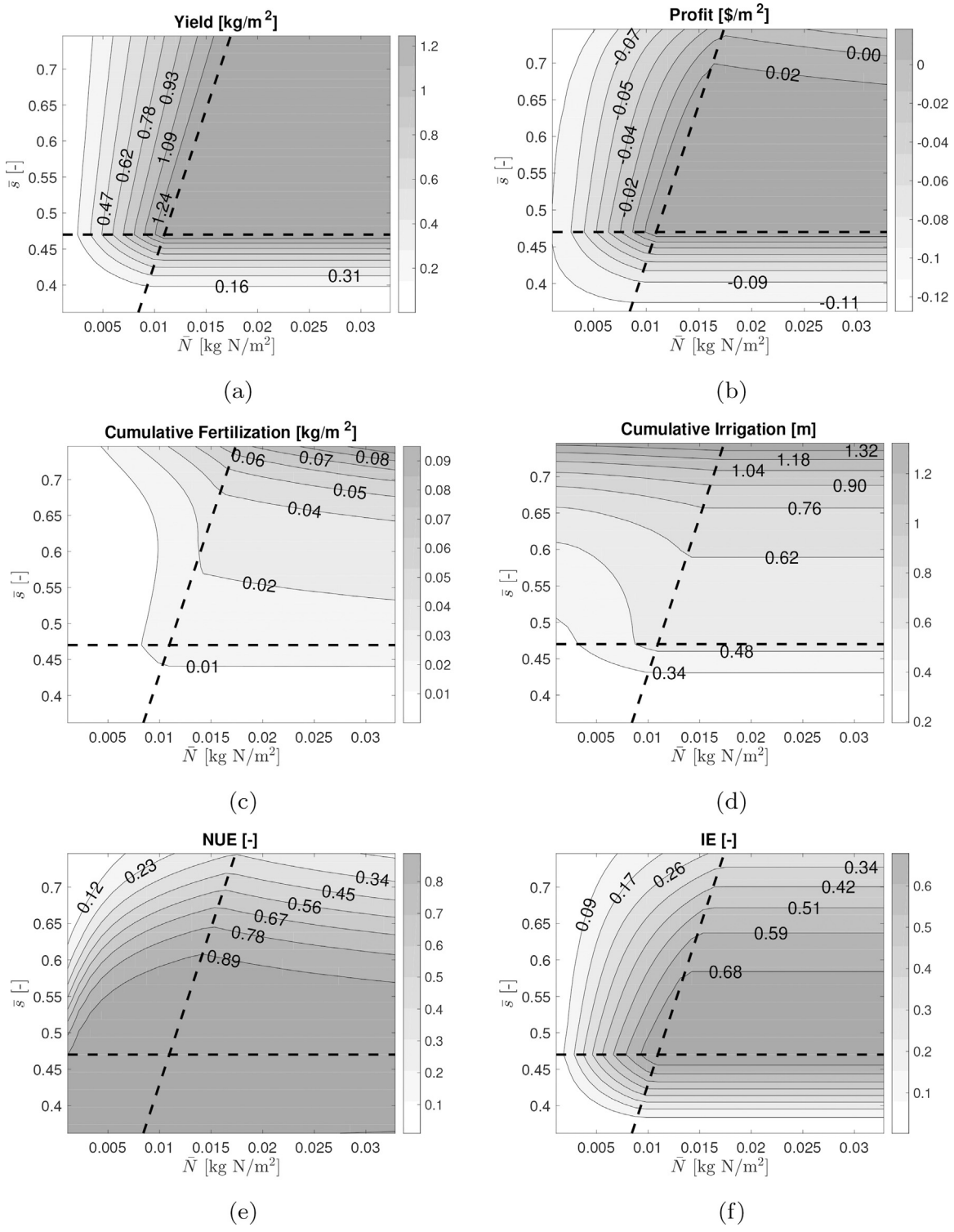

Fig. 8. Response to the necessary rates of irrigation and fertilization to keep S and N at the designated constant values of (a) crop yield, (b) profit, (c) cumulative fertilization [kg/m^2], (d) cumulative irrigation [m], (e) nitrogen use efficiency (NUE), the cumulative nitrogen uptake as a fraction of total fertilization, and (f) irrigation efficiency (IE), the cumulative transpiration as a fraction of the total irrigation. The horizontal dashed line represents the S^* threshold, while the diagonal dashed line is the η_c limit. All figures are for deterministic conditions (i.e., no stochastic forcing in the rainfall).

and is an important metric by which to judge fertilization strategies. Similarly, we can define the irrigation efficiency (IE) as the ratio of the irrigation water applied to the amount which is transpired by the crop. These two values are shown in Fig. 8e and f, respectively, as a function of the mean soil moisture and mean soil nitrogen. Each of the panels in Fig. 8 sheds light on a different consideration for the optimal use of water and nitrogen resources. However, the common thread between them is that in each case, the 'best' scenario from the perspective of using water and nitrogen resources in the most efficient manner (i.e. maximizing IE and NUE to produce the highest possible yield and profit), occurs at the intersection of the S^* and η_c lines. At this point neither water nor nitrogen is lim-

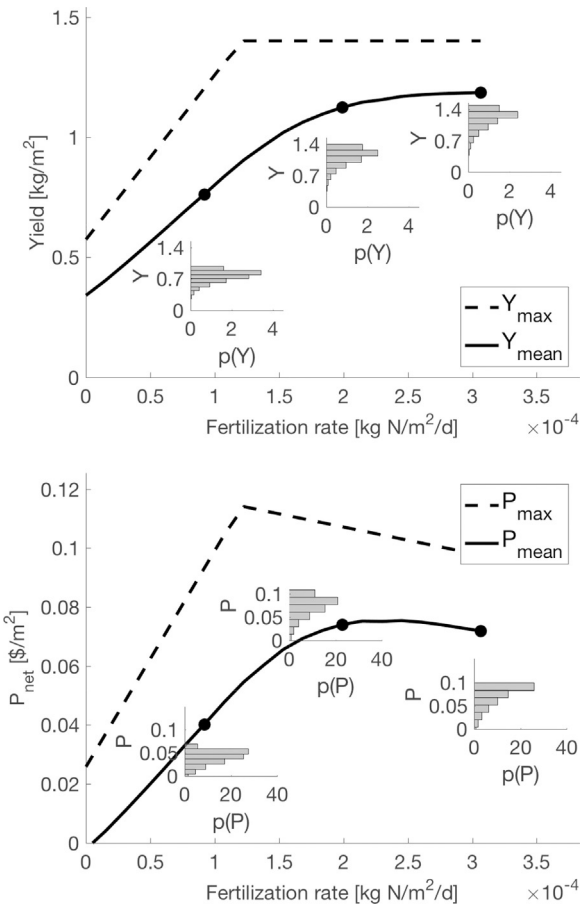

Fig. 9. Yield (top) and profit (bottom) as a function of the constant fertilization rate. The dashed line represents a theoretical maximum while the solid line is the mean of many simulations. The inset plots show the numerical probability density functions at each point.

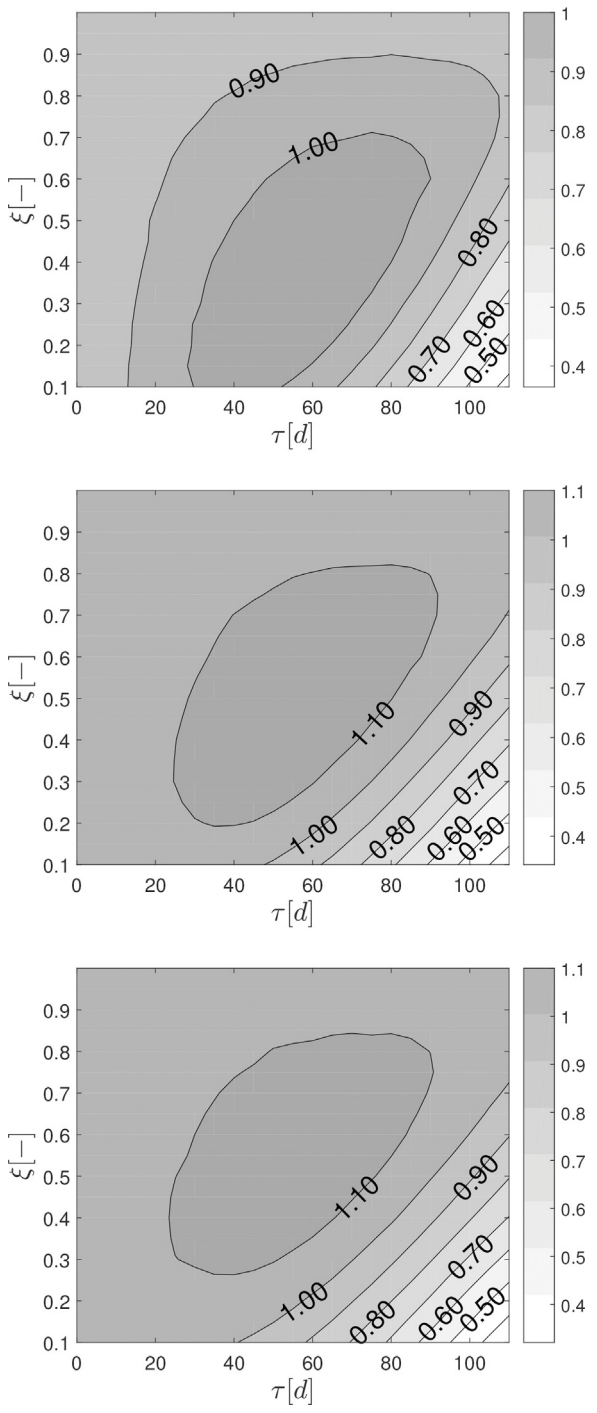

Fig. 10. Crop yield as a function of ξ, the fraction of the total fertilization amount which is applied at the beginning of the growing season, and τ, the time between the first and second fertilizer applications, for three soil depths: $Z = 33$ cm (top), $Z = 67$ cm (middle), and $Z = 100$ cm (bottom). In this figure, microirrigation was used to prevent the soil moisture from dropping below S^*, and therefore the crop can experience only nitrogen stress, not water stress.

iting, and no extra irrigation or fertilization beyond what is needed to keep the system at these S and N values is used. However, with the addition of the random rainfall in the next section, additional concerns such as the robustness of the optimal strategies under stochastic forcing must also be considered.

5.1. Optimization under stochastic rainfall conditions

Random hydroclimatic forcing adds uncertainty to the expected value of the objective function. This is illustrated in Fig. 9, which shows the numerical probability distribution functions of yield and profit for varying fertilization rates. Note that as the fertilization rate increases, both the mean of the yield and its variance increase. The mean increases because the higher fertilization rates lead to less likelihood that the crop will experience a shortage of nitrogen, while the variance increases because the field of possible yields expands – the extra nitrogen raises the maximum possible yield, while a low-rainfall growing season could still occur, so lower yields are still possible. The probability distributions in Fig. 9 highlight the fact that under stochastic rainfall conditions, the question of optimization must be examined from a probabilistic point of view. Unlike in the previous section, optimal strategies for a system undergoing stochastic forcing must attempt to maximize profit while also being robust to adverse conditions, such as drought or flood years. This necessarily involves tradeoffs between maximizing yield and profit on the one hand and mitigating risk on the other. For example, we point out that in the bottom of Fig. 9, the theoretical maximum (which refers to the value which would be obtained if the crop experienced no water stress and took up as much N as possible) for profit (dashed line) occurs at a much lower fertilization rate than the maximum of the actual profit under stochastic rainfall conditions (black line), demonstrating in a simple way the necessity of accounting for the possibility of adverse conditions. A detailed analysis of such concerns is beyond the scope of this work, though we point out that many studies have examined the

related concept of resilience in ecological and social systems (see for example Walker et al. (2004)).

In order to examine the impact of stochastic forcing on optimal fertilization, we first suppose that the total fertilization over the course of a growing season F_t (the value of which can be found in Table 1) is to be divided into two treatments, which corresponds to a typical fertilization schedule for corn (e.g., Brady et al. (1996)). The placement of the fertilizer applications in time is varied by changing the fraction of F_t which is applied in each application and the amount of time between the two applications. In order to focus on optimal fertilization timing and amounts under stochastic conditions, we do not consider the other potential degrees of freedom in the fertilization scheduling, such as varying the total amount of fertilizer used or using more than two applications. The effect of varying ξ and τ (the fraction of F_t in the first application and the time between the first and second applications, respectively) on crop yield can be seen in Fig. 10, which shows the yield response to varying ξ and τ for three different soil depths. Larger soil depths lead to less variation in S and thus less percolation and leaching, thereby increasing the fraction of $\xi - \tau$ space in which higher yields can occur. The exact location of the peak yield is a result of the balance which maximizes the uptake of nitrogen and minimizes the loss due to leaching.

6. Conclusion

We have presented a dynamical system for crop evolution, based on the AquaCrop model (Steduto et al., 2009) and minimal models for soil moisture and nitrogen cycling used in ecohydrology (Rodríguez-Iturbe and Porporato, 2004). It includes canopy cover, soil moisture, and soil nitrogen as its main state variables and tracks fluxes of water and nitrogen from evapotranspiration, nitrogen uptake, and leaching. This parsimonious model, with its reduced number of parameters, may be useful for evaluating the impact of different fertilization and irrigation strategies as well as different precipitation and climate regimes on crop yield, expected profit, and other outputs of interest. A simple objective function was used to compare optimal strategies of fertilization and irrigation.

The results highlight the importance of considering, from a quantitative and theoretical point of view, the optimization of these agricultural inputs, and also provide a direct connection with climate parameters. Hydroclimatic forcing is a major driver of variability in agricultural systems, which has implications not only for crop yield and profitability but also for environmental impact. The model developed here is capable of characterizing the variability in the model outputs and provides a link to the random processes which drive this variability.

Agroecosystems cover a large portion of the Earth's surface and provide essentially all of the global food supply. It is thus crucial to have a more complete understanding of the fluxes of water and nutrients in such systems, and their dependence on potentially changing hydroclimatic inputs and human activities. To this regard, the model presented here may be useful to explore scenarios and generate hypotheses. The framework can be extended in a number of directions. In order to emphasize the dynamical systems point of view, the model presented here necessarily included certain simplifications. However, including more detailed plant and soil models and performing a comparison with more complete crop models would provide firmer ground from which to make predictions. Moreover, the model could easily account for periodic seasonal variations in temperature, radiation, or rainfall, which alter the water and nutrient cycles and therefore the optimal fertilization and irrigation strategies. Finally, the nature of agroecosystems is that they are heavily intertwined with human activities (e.g., Sivapalan et al. (2012), Porporato et al. (2015), Assouline et al. (2015)), suggesting the need to couple models for ecological systems and landscape evolution with social and behavioral models (e.g., harvesting in Parolari and Porporato (2016) and Pelak et al. (2016)). We hope that these considerations will be accounted for in future contributions, providing a quantitative framework for the sustainable use of soil and water resources while ensuring food security.

Acknowledgements

We acknowledge financial support from the National Science Foundation (DGE-1068871, NSF-EAR-0838301, NSF-EAR-1331846, and NSF-EAR-1316258) and the Duke Wireless Intelligent Sensor Networks (WISeNet) Integrative Graduate Education and Research Training (IGERT) program, the US Department of Defense through the NDSEG Fellowship program, and the European Union's Horizon 2020 research and innovation program under the Marie Sklodowska-Curie grant agreement ECO.G.U.S. (701914).

References

Aggarwal, P.K., Kalra, N., Chander, S., Pathak, H., 2006. InfoCrop: a dynamic simulation model for the assessment of crop yields, losses due to pests, and environmental impact of agro-ecosystems in tropical environments. I. Model description. Agric. Syst. 89, 1–25.

Allen, R.G., Pereira, L.S., Raes, D., Smith, M., et al., 1998. FAO Irrigation and Drainage Paper 56: Crop Evapotranspiration (Guidelines for Computing Crop Water Requirements).

Assouline, S., Russo, D., Silber, A., Or, D., 2015. Balancing water scarcity and quality for sustainable irrigated agriculture. Water Resour. Res. 51, 3419–3436.

Bender, R.R., Haegele, J.W., Ruffo, M.L., Below, F.E., 2013. Nutrient uptake, partitioning, and remobilization in modern, transgenic insect-protected maize hybrids. Agron. J. 105, 161–170.

Boote, K.J., Jones, J.W., Hoogenboom, G., 1998. Simulation of Crop Growth: CROPGRO Model. Marcel Dekker, Inc.

Brady, N.C., Weil, R.R., et al., 1996. The Nature and Properties of Soils, 11th ed. Prentice-Hall, Inc.

Brisson, N., Gary, C., Justes, E., Roche, R., Mary, B., Ripoche, D., Zimmer, D., Sierra, J., Bertuzzi, P., Burger, P., et al., 2003. An overview of the crop model STICS. Eur. J. Agron. 18, 309–332.

Brooks, R., Corey, T., 1964. Hydraulic Properties of Porous Media. Hydrology Papers. Colorado State University.

Brutsaert, W., Chen, D., 1995. Desorption and the two stages of drying of natural tallgrass prairie. Water Resour. Res. 31, 1305–1313.

Clapp, R.B., Hornberger, G.M., 1978. Empirical equations for some soil hydraulic properties. Water Resour. Res. 14, 601–604.

Doorenbos, J., Kassam, A., 1998. FAO Irrigation and Drainage Paper 33: Yield Response to Water.

Guswa, A.J., Celia, M., Rodriguez-Iturbe, I., 2002. Models of soil moisture dynamics in ecohydrology: a comparative study. Water Resour. Res. 38.

Hsiao, T.C., Heng, L., Steduto, P., Rojas-Lara, B., Raes, D., Fereres, E., 2009. AquaCrop – the FAO crop model to simulate yield response to water: III. Parameterization and testing for maize. Agron. J. 101, 448–459.

Irmak, S., Rudnick, D.R., 2014. Corn Soil–Water Extraction and Effective Rooting Depth in a Silt Loam Soil. Technical Report. Institute of Agriculture and Natural Resources, University of Nebraska-Lincoln Extension.

Jeuffroy, M.H., Recous, S., 1999. Azodyn: a simple model simulating the date of nitrogen deficiency for decision support in wheat fertilization. Eur. J. Agron. 10, 129–144.

Johnson, I., Parsons, A., 1985. A theoretical analysis of grass growth under grazing. J. Theor. Biol. 112, 345–367.

Kelliher, F., Leuning, R., Raupach, M., Schulze, E.D., 1995. Maximum conductances for evaporation from global vegetation types. Agric. For. Meteorol. 73, 1–16.

Laio, F., Porporato, A., Fernandez-Illescas, C., Rodriguez-Iturbe, I., 2001a. Plants in water-controlled ecosystems: active role in hydrologic processes and response to water stress: IV. Discussion of real cases. Adv. Water Resour. 24, 745–762.

Laio, F., Porporato, A., Ridolfi, L., Rodriguez-Iturbe, I., 2001b. Plants in water-controlled ecosystems: active role in hydrologic processes and response to water stress: II. Probabilistic soil moisture dynamics. Adv. Water Resour. 24, 707–723.

Lamm, F., Stone, L., O'Brien, D., 2007. Crop production and economics in Northwest Kansas as related to irrigation capacity. Appl. Eng. Agric. 23, 737–745.

Makeham, W.M., 1860. On the law of mortality and construction of annuity tables. Assur. Mag. J. Inst. Actuar. 8, 301–310.

Manzoni, S., Porporato, A., 2007. A theoretical analysis of nonlinearities and feedbacks in soil carbon and nitrogen cycles. Soil Biol. Biochem. 39, 1542–1556.

Manzoni, S., Porporato, A., D'Odorico, P., Laio, F., Rodriguez-Iturbe, I., 2004. Soil nutrient cycles as a nonlinear dynamical system. Nonlinear Process. Geophys. 11, 589–598.

Mau, Y., Porporato, A., 2015. A dynamical system approach to soil salinity and sodicity. Adv. Water Resour. 83, 68–76.
Murray, J.D., 2002. Mathematical Biology: An Introduction, 3rd ed. Springer-Verlag, New York, NY.
National Atmospheric Deposition Program (NRSP-3), 2017. NADP Program Office, Illinois State Water Survey. University of Illinois, Champaign, IL.
Parolari, A.J., Porporato, A., 2016. Forest soil carbon and nitrogen cycles under biomass harvest: stability, transient response, and feedback. Ecol. Model. 329, 64–76.
Pelak, N.F., Parolari, A.J., Porporato, A., 2016. Bistable plant–soil dynamics and biogenic controls on the soil production function. Earth Surf. Process. Landf. 41, 1011–1017.
Porporato, A., D'Odorico, P., Laio, F., Rodriguez-Iturbe, I., 2003. Hydrologic controls on soil carbon and nitrogen cycles. I. Modeling scheme. Adv. Water Resour. 26, 45–58.
Porporato, A., Dodorico, P., Laio, F., Ridolfi, L., Rodriguez-Iturbe, I., 2002. Ecohydrology of water-controlled ecosystems. Adv. Water Resour. 25, 1335–1348.
Porporato, A., Feng, X., Manzoni, S., Mau, Y., Parolari, A.J., Vico, G., 2015. Ecohydrological modeling in agroecosystems: examples and challenges. Water Resour. Res. 51, 5081–5099.
Raes, D., Steduto, P., Hsiao, T.C., Fereres, E., 2009. AquaCrop – the FAO crop model to simulate yield response to water: II. Main algorithms and software description. Agron. J. 101, 438–447.
Rhoads, F., Yonts, C., 2000. Irrigation scheduling for corn – why and how. In: National Corn Handbook. Water Management (Irrigation). US Department of Agriculture (USDA).
Ritchie, J., Singh, U., Godwin, D., Bowen, W., 1998. Cereal growth, development, and yield. In: Understanding Options for Agricultural Production. Springer, pp. 79–98.
Ritchie, J.T., 1972. Model for predicting evaporation from a row crop with incomplete cover. Water Resour. Res. 8, 1204–1213.
Rodríguez-Iturbe, I., Porporato, A., 2004. Ecohydrology of Water-Controlled Ecosystems: Soil Moisture and Plant Dynamics. Cambridge University Press.
Rodríguez-Iturbe, I., Porporato, A., Ridolfi, L., Isham, V., Coxi, D., 1999. Probabilistic modelling of water balance at a point: the role of climate, soil and vegetation. Proc. R. Soc. Lond. A: Math. Phys. Eng. Sci., 3789–3805.
Schaffer, B.E., Nordbotten, J.M., Rodriguez-Iturbe, I., 2015. Plant biomass and soil moisture dynamics: analytical results. In: Proc. R. Soc. A., pp. 2050179.
Sivapalan, M., Savenije, H.H., Blöschl, G., 2012. Socio-hydrology: a new science of people and water. Hydrol. Process. 26, 1270–1276.
Steduto, P., Hsiao, T.C., Raes, D., Fereres, E., 2009. AquaCrop – the FAO crop model to simulate yield response to water: I. Concepts and underlying principles. Agron. J. 101, 426–437.
Stöckle, C.O., Donatelli, M., Nelson, R., 2003. Cropsyst, a cropping systems simulation model. Eur. J. Agron. 18, 289–307.
Strogatz, S.H., 2014. Nonlinear Dynamics and Chaos: With Applications to Physics, Biology, Chemistry, and Engineering. Westview Press.
Thornley, J., Bergelson, J., Parsons, A., 1995. Complex dynamics in a carbon–nitrogen model of a grass–legume pasture. Ann. Bot. 75, 79–94.
Thornley, J., Cannell, M., 1992. Nitrogen relations in a forest plantation–soil organic matter ecosystem model. Ann. Bot. 70, 137–151.
Thornley, J., Verberne, E., 1989. A model of nitrogen flows in grassland. Plant Cell Environ. 12, 863–886.
Thornley, J.H., Johnson, I.R., 1990. A Mathematical Approach to Plant and Crop Physiology. The Blackburn Press.
Tilman, D., Wedin, D., 1991. Oscillations and chaos in the dynamics of a perennial grass. Nature 353, 653.
Vico, G., Porporato, A., 2010. Traditional and microirrigation with stochastic soil moisture. Water Resour. Res. 46.
Vico, G., Porporato, A., 2011a. From rainfed agriculture to stress-avoidance irrigation: I. A generalized irrigation scheme with stochastic soil moisture. Adv. Water Resour. 34, 263–271.
Vico, G., Porporato, A., 2011b. From rainfed agriculture to stress-avoidance irrigation: II. Sustainability, crop yield, and profitability. Adv. Water Resour. 34, 272–281.
Walker, B., Holling, C.S., Carpenter, S., Kinzig, A., 2004. Resilience, adaptability and transformability in social–ecological systems. Ecol. Soc., 9.
Wallach, D., Makowski, D., Jones, J.W., 2006. Working with Dynamic Crop Models: Evaluating, Analyzing, Parameterizing, and Applications. Elsevier.